Experimental Investigation on Mechanical Properties of thick dissimilar light weight material joints fabricated by friction stir welding

R. Venkateswara Rao[1], M. Senthil Kumar[2]

[1]Asst Professor, Vignana Bharathi Institute of Technology, Hyderabad, Telangana- 501301, India

[1,2]School of Mechanical and Building Sciences, Vellore Institute of Technology, Chennai- 600127, India

E-mail: [1]rvraomechanical@gmail.com, [2]senthil.km@vit.ac.in

DOI : 10.22486/iwj.v53i4.203671

ORCID: R. Venkateswara Rao : https://orcid.org/0000-0001-6458-2327

ORCID: M. Senthil Kumar : https://orcid.org/0000-0002-6369-2898

Abstract

Friction stir welding (FSW) is a solid state technique used to join aluminum alloys effectively compared with other conventional welding methods. AA6061/AA2014 Al-alloys in dissimilar combination were processed for welding because they have significant demand in various engineering applications. The process parameters chosen for welding are tool rotational speed (710 to 1120 rpm), weld speed (20 to 40 mm/min) and pin profile (Triangular, Square and Pentagon) were arranged in L9 orthogonal array. The weld joint properties such as hardness and tensile strength were tested as per ASTM standard. The microstructure of weld profile was studied with optical, scanning electron microscopy. The welds processed at 900-20-S were exhibits higher properties such as UTS, YS and hardness as 191, 170 MPa, 110 HV respectively.

Keywords: Friction stir welding; AA6061/AA2014Al-alloys; weld parameters; weld properties.

1.0 Introduction

Welding is the most widely used fabrication technique in manufacturing industry. Friction stir welding (FSW) is a new welding method invented by Thomas WM, at TWI UK, in 1991 to overcome the fusion welding problems [1-2]. Mishra et al. experimented [3] on few similar and dissimilar materials and identified some unsolved critical issues. Few researchers extend the limits of FSW in welding of different materials like Al-Cu [4], Cu-Al [5], Al-Mg [6], and plastics [7]. The material flow during the process was analytical studied [8] and the key notations reported in FSW process was shown in **Fig.1**.

FSW process is extensively used in various industrial applications from the invention, it is highly recommended technique for joining current and future advanced materials. In this process, shoulder/workpiece interface causes to generate the frictional heat results in plastic deformation of the work

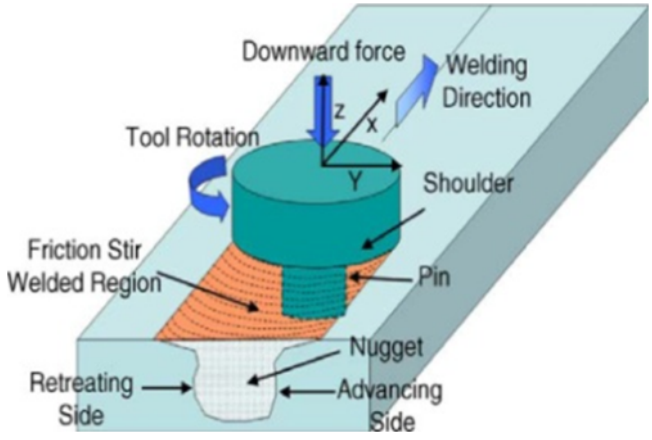

Fig.1 : Schematic view of FSW Process

piece. Welding parameters have an impact on the material flow, heat generation which effected the weld strength. The rotational, weld speeds of the tool and pin profile geometry affect the temperature and plastic flow field [9]. Weld joint strength was increases with increase in TRS was studied and reported in dissimilar AA7075-AA2024 Al-alloys FSW joints [10]. The weld quality was evaluated by hardness of the joint, relationship between peak temperature and hardness profile at stir zone was investigated on AA6061-AA7075 Al-alloy joints [11]. The impact of weld speed on joint strength was studied in dissimilar AA6061-T6/AA7075-T6 Al-alloys joints. The welds fabricated at different weld speeds of 80, 100, 120 mm/min, where defect-free and superior strength joints were produced at 120 mm/min [12]. The effect of TRS on stir zone of dissimilar AA601/AA7050 Al-alloy joints revealed that, degree of material transfer g was influenced by the tool rotational speed [13].The study report on AA6061/AA5086 Al-alloy revealed that, welds fabricated with threaded cylindrical pin profiles exhibits better mechanical properties than welds fabricated with other welds [14]. Another study reported that, dissimilar AA6061/AA5010 Al-alloy welds made with square pin profile exhibits superior strength compared to cylindrical pin profiles [15]. The study reported on dissimilar AA6061/AA2014 Al-alloy revealed that, joints fabricated by hybrid square pin profiles exhibit good material flow than other welds [17].

Fabrication of different grade materials with FSW is a challenging task to the researchers and manufacturers. The present study aimed to investigate the influence of polygonal pin profiles on weld joint and mechanical properties of 8 mm thick dissimilar AA6061/AA2014 Al-alloy weldments. The fabricated materials combination have applications in fabricate the truck frames, aircraft structures, automotive parts, marine and ship building, storage tanks and railroad cars etc.

2.0 Experimental Procedure

Flat plates ofAA6061/AA2014 Al-alloys in 8 mm thick were chosen for make the butt joints. The parent materials chemical composition was reported [17]. Initially the specimens were chemically treated to remove grease, dirt particles at the weld site. The process is carried out on FSW machine with FANUC controller as shown in **Fig. 2**.

Process parameter and their levels were designed by using a L9 orthogonal array (OA). The trail runs were carried out at a speed of 710-900-1120 rpm, feed rate of 20-31.5-40 mm per min, Pin profiles (T, S, and P). The harnesses was tested on hardness testing machine with a working load of 110Kgf and a dwell period of 10sec. Tensile test was conducted as per ASTM E8 on precision universal testing machine (SHIMADZU) have a test load of 50KN at a cross head velocity of 1 mm/min. Microstructure analysis was studied with optical, scanning electron microscopy.

Fig. 2 : Experimentation setup

2.1 Tool material and profiles

In the first stage, the tool is stirred and pin shape is plunged into the workpiece. The non-consumable tool material used for this experiment is AISI-H13 tool steel. The non-consumable rotating tool consists of two main parts like shoulder and pin. Tool shoulder can play a key role to produce a frictional heat to soften the material in and around the pin. During the process, the tool inserts on abutted surfaces of clamped plates and traversed along the weld joint from advanced to retreating side, where the material will undergo plastic deformation. The tool material used for fabricated the Al-alloy joints was used by many authors and also published in [17].

Though different pin profiles were experimented, polygonal profiles namely triangle, square and pentagonal profiles permits the better material transfer and they were made with AISI H-13 tool steel. The tool dimensions taken as per the ratio of shoulder to pin dimensions [16] were given in **table 1**.

Table 1: Tool pin profile dimensions

S No	Tool type	Shoulder diameter(mm)	Pin diameter(mm)	Pin length (mm)
1	Triangle	24	8	7.8
2	Square	24	8	7.8
3	pentagon	24	8	7.8

Photographs of the fabricated pin profiles were shown in **Fig. 3**,

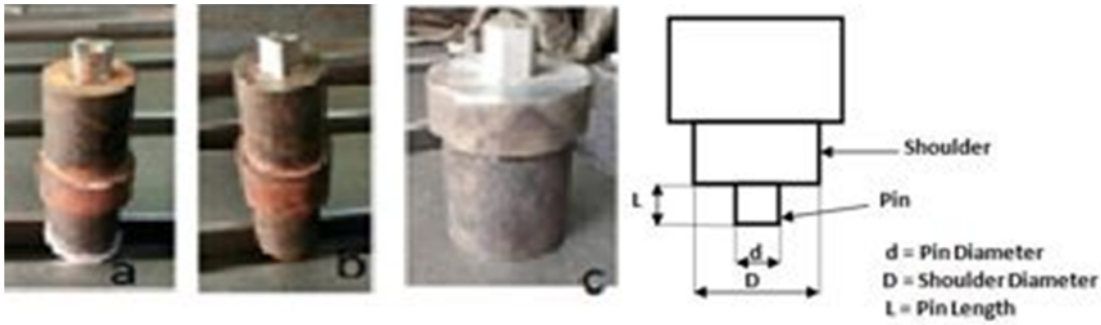

Fig. 3 : (a) Triangle (b) Square and (c) pentagonal (d) tool dimensions

3. 0 Results and Discussion

3.1 X-ray radiography test

The weld surfaces were checked by X-ray radiography (NDT) as per ASTM E505-15 standard by using AGFA-D7 film to identify the structural defects in weldment. The welds made with different pin profiles processed at 900 rpm were experienced by radiography test, which not shows any defect same was shown in **Fig. 4.**

3.2 Temperature Measurement

During the FSW process, generated frictional heat at the shoulder/workpiece contact is more and the material will undergone plastic deformation. The temperature profile during the process is measured with the help of an infrared thermometer. The heat generated in the process is responsible for softening the material at the weld region which reduced the thermomechanical stresses on the tool during the process.

In FSW process, the contact area between pin profile and the weld surfaces were responsible to generate the frictional heat during the process. The estimated heat generated during the process was calculated by using the following equations.

$$Q_{total} = 2/3\pi\rho\mu\omega\ (R^3 shoulder - R^3 pin)\ (Sliding) \quad (1)$$

$$Q_{total} = 2/3\pi T\omega\ (R^3 shoulder - R^3 pin)\ (Sticking) \quad (2)$$

Where ω is the weld speed, $R_{shoulder}$ is the shoulder radius, R_{pin} is the pin radius and T is the torque.

The heat input was primarily estimated by using the equation is given by

$$Q = \eta \frac{2\pi\omega T}{\nu} \quad (3)$$

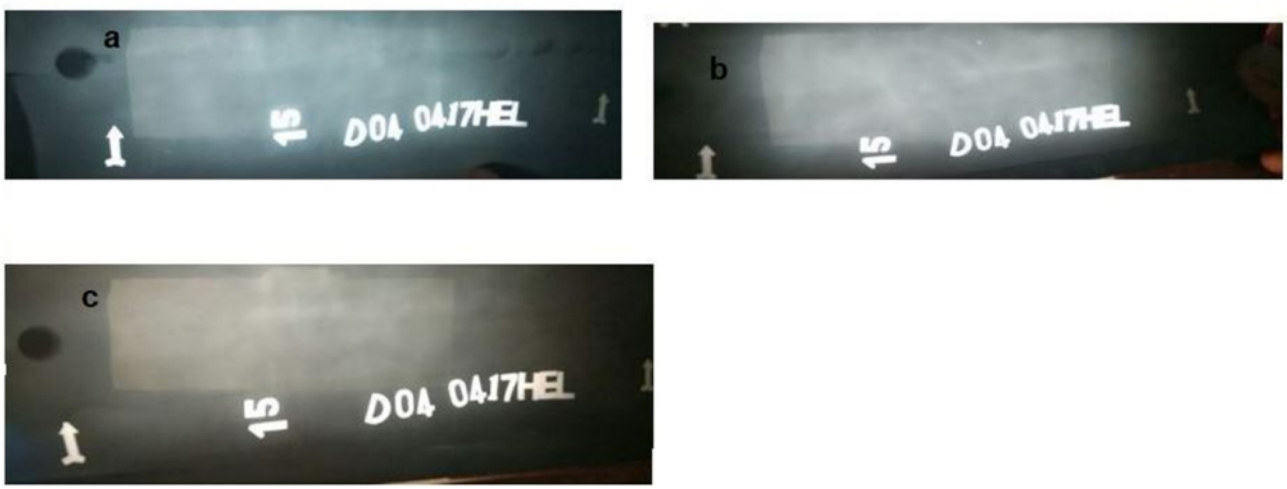

Fig. 4 : Welds processed with different pins (a) Triangle (b) Square and (c) pentagon

The terms used in equation 3 were clearly defined [16], same was reported.

The heat generated during the process was measured in terms of temperature with the help of IR thermometer. The temperature transferred from NZ to ends of the weld plates was varied. The varied temperature measured at various regions was shown in **Fig. 5**.

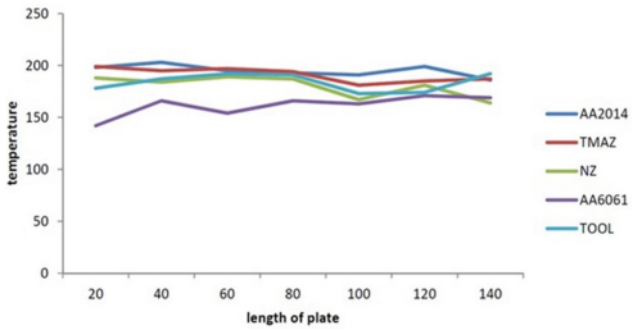

Fig. 5 : Temperature profile of weldment along the weld joint.

3.3 Microstructure

The weldments were cut across the weld joint in order to view the microstructure. The specimens were prepared by polishing till a scratch free mirror-like image is got, further they are etched with Keller's reagent (95 ml of water, 2.5 ml of nitric acid, 1.5 ml of hydrofluoric acid and 1 ml of hydrochloric acid). The microstructures of etched specimens were observed under an optical microscope. In FSW process, the plastically deformed material in the weld zone was experienced by the thermo-mechanical cycle. The weld zone cross-section have the fine grained structure, in dissimilar materials welding, the analysis of microstructure is a complex due to heterogeneous properties of materials. The microstructure so obtained shows grains, grain boundaries are shown in **Fig. 6** that have intermetallic particles, and some grains are elongated. The microstructure analysis has reported that TMAZ consists coarser and elongated grains because of the heat produced by the tool shoulder during rotation. The microstructures captured at different locations were shown in **Fig. 6**.

3.4 SEM Analysis

To study the microstructure at higher magnification specimens were subjected to SEM (ZEISS model) and EDAX. The microstructure at the weld zone was asymmetric due to different chemical composition of the base materials. It seen from SEM images, the welds processed with square pin profiles have good material mixing. Whereas the elements magnesium and silicon form Mg_2Si compound shown as bright regions which not dissolve in parent materials shown in **Fig 7**. This leads to conclude that dark lamellar originates from AA2014 (Al–Cu alloy) and the bright lamellar from AA6061 (Al–Si–Mg alloys). The SEM image of the sample fabricated with polygon pin profiles and processed at 900 rpm is shown in **Fig. 7**.

EDAX analysis showed in **Fig. 8** addresses the secondary-phase IMCs in the form of Mg_2Si, consists at nugget zone. In the NZ, an average composition close to that of the alloy 2014 was found in EDAX. The EDAX confirmed the elemental composition of the welds at nugget zone. EDAX profile showed that NZ have less Cu content than base materials. The compounds like $CaCO_3$, SiO_2, Al_2O_3, KCl were present in the NZ. The composition at the weld zone was found out with EDAX and it was shown in **Fig. 8**.

3.6 Mechanical properties

The microstructure variations in and around the weld zone can lead to change in tensile strength of the weldment. The joint efficiency was calculated as

$$\text{Joint efficiency} = \frac{\text{Weld failure load}}{\text{Base material failure load}} \times 100 \qquad (4)$$

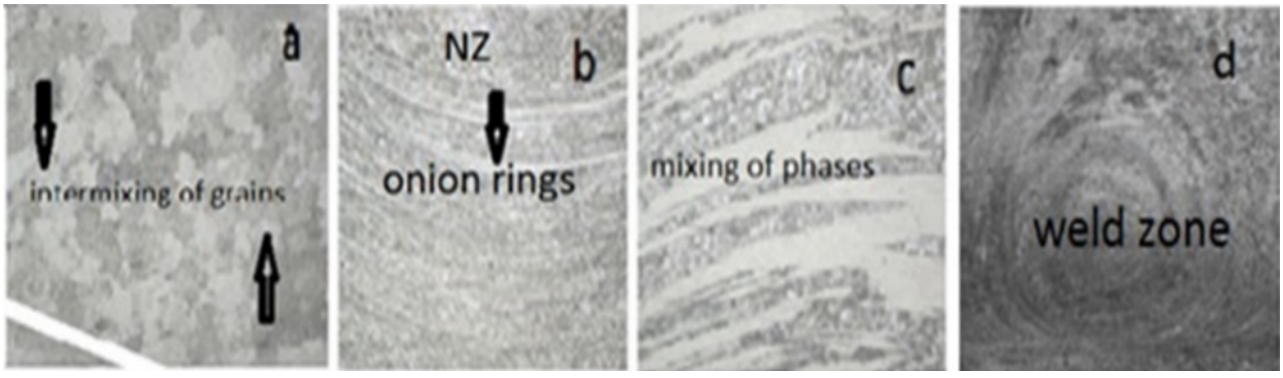

Fig. 6 : Photographs of microstructures

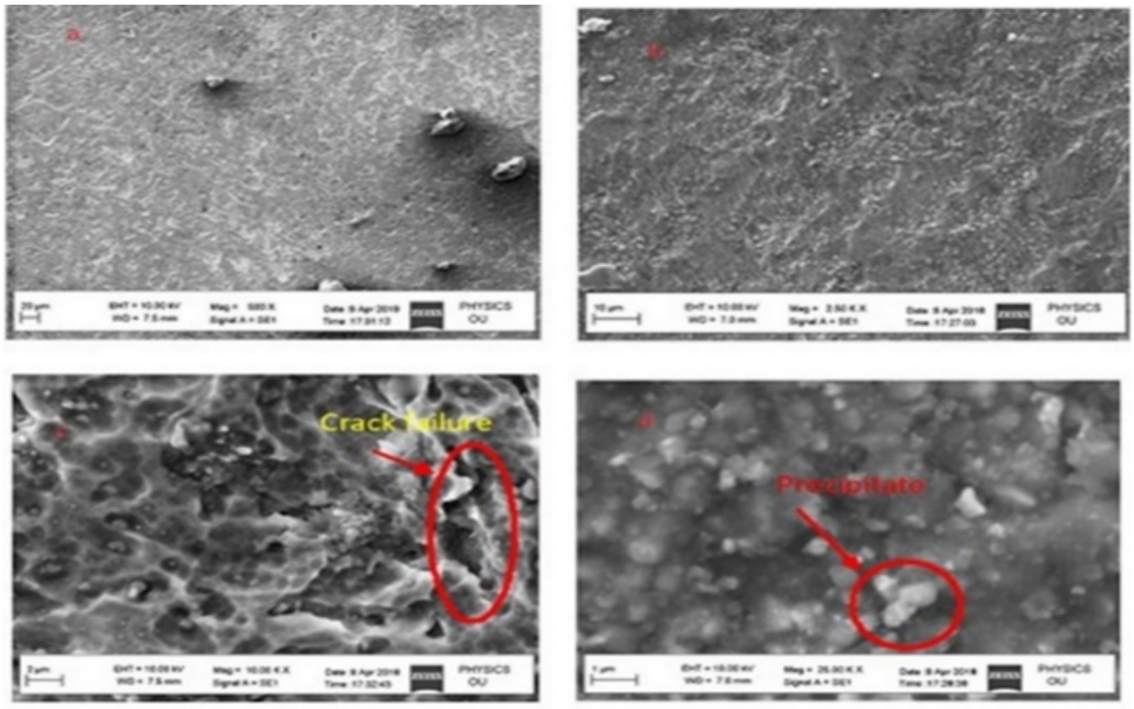

Fig. 7 : SEM images at various magnification levels

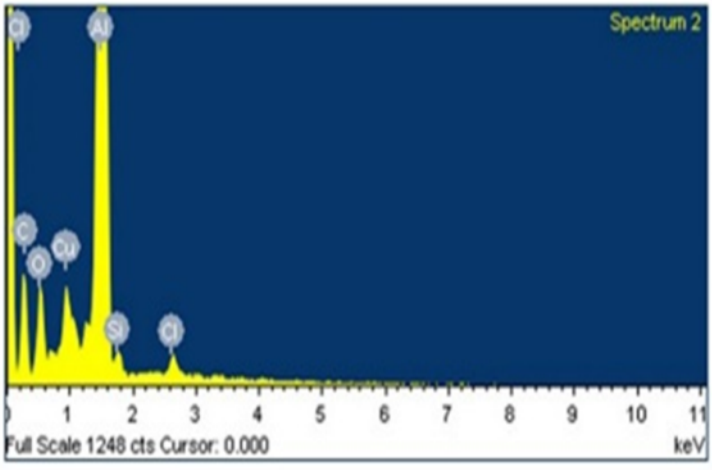

Element	Wt %	At %
C	17.24	31.26
O	5.60	7.62
Al	73.25	59.12
Si	0.87	0.68
Cl	1.04	0.64
Cu	1.99	0.68
Total	100%	100%

Fig. 8 : EDAX profile

3.6.1 Hardness

The hardness of the weld joint was determined from mid to parent material. The hardness variation found either side of the weld joint was non-symmetric because of difference in parent material properties. The hardness distribution of the FSW joints depends on the IMCs and distribution of the particles in the stir zone. In weld condition, the micro hardness profile fluctuated across the welded joint, and minimum hardness value found in HAZ on the AA6061 side. The hardness is minimum due to precipitation in the nugget zone of the AA6061 side. The less hardness observed in the HAZ is due to the IMCs may form Mg_2Si, SiO_2 compound on the AA6061 side. The hardness values observed were 80 to125 HV from NZ to HAZ. The weld zone hardness varied between 80 to 110 HV. Hardness test conducted on the transverse section of welded samples with a spacing of 5 mm and a load of 110 Kgf with a dwell period of 10 sec. The welds fabricated with polygonal pin profiles processed at 900 rpm exhibits differences in hardness along the weld line was shown in **Fig. 9**.

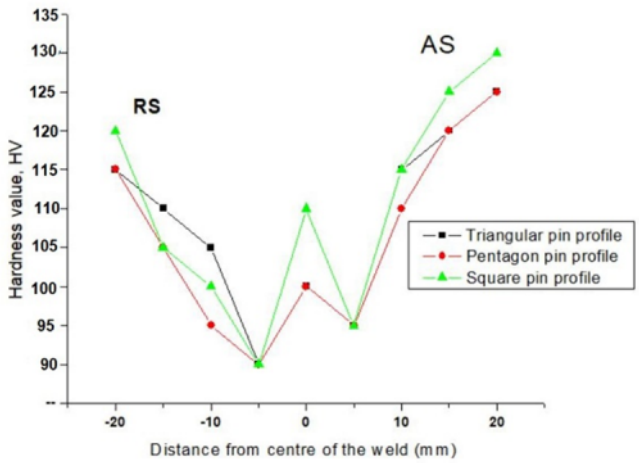

Fig. 9 : Hardness profile of weld joints processed at different pin profiles

3.6.2 Tensile Strength

Tensile test samples were prepared as per the standard of ASTM E8/ASTM B557. The test specimen shape was cut by wire EDM machine in order to get accurate dimensions shown in **Fig. 10 (a)**, the test was conducted on the precision universal testing machine (SHIMADZU) at a test load of 50 KN and a cross-head velocity of 1 mm/min. The test results revealed that the failure region was noticed on weaker material side rather than other side of the welded joint. The NZ was composed of equiaxed fine grains and TMAZ is having coarse bent recovered grains. The tensile test failure region on weaker material side was shown in **Fig. 10(b)**.

The fracture location is between WN and TMAZ are on AS. Maximum UTS and YS values were recorded as 191 MPa and 170 MPa respectively. As per (AWS D17) specifications, the joint efficiency factor for aerospace applications is 0.6 to 0.7, which is achieved in this experiment. Hence, the fabricated joints were recommended for various structural applications where the above properties are required. The results observed from the experiment were tabulated in **table 2**.

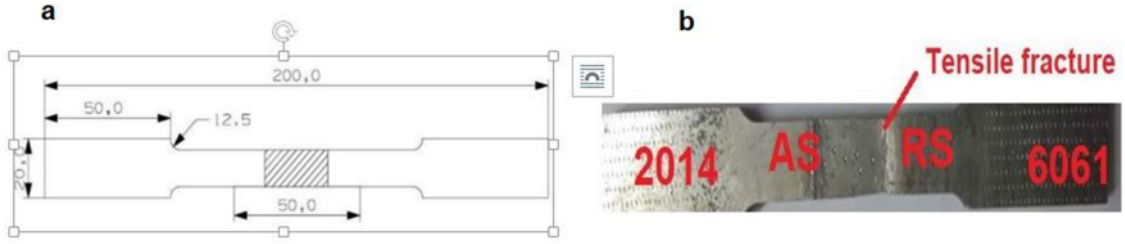

Fig.10 : Tensile test sample specifications

Table 2 : Process parameters with response values

TRS	WS	Pin Profile	UTS	Joint efficiency factor	YS	HV
710	20	T	180	180/270=0.66	165	99
710	31.5	S	150	150/270=0.55	105	98
710	40	P	182	182/270=0.67	168	99
900	20	S	191	191/270=0.70	170	110
900	31.5	P	148	148/270=.54	115	95
900	40	T	150	150/270=0.55	98	96
1120	20	P	125	125/270=0.46	94	92
1120	31.5	T	154	154/270=0.57	93	90
1120	40	S	97	97/270=0.35	93	92

4.0 Conclusion

In this study, dissimilar Al-alloys were joined and the following conclusions were drawn:

- Polygonal pin profiles were successfully fabricate the AA2014/AA6061 dissimilar materials with good strength.
- SEM Microstructure showed that very fine grains and structured onion rings in NZ, which defines good material mixing between the two materials.
- The highest tensile strength reported as 191 MPa. The highest hardness was reported as 110 HV.
- AWSD17 requirement acquired with a joint efficiency factor 0.7.

Acknowledgement

The Authors wish to express thank to the Dean VIT Chennai for their acceptance for experimentation. Authors are also thankful to the principal, VBIT-Hyderabad and FIST for support to this work.

The present paper is a revised version of an article presented in the International Conference on Advancements in Mechanical Engineering (ICAME-2020) held at Aliah University, Kolkata on January 16-18 2020.

References

[1] Thamos WS and Nicholas ED (1997); Friction stir welding for the transportation industries, Materials and Design, 18(4-6), pp. 269-273.

[2] Thamos WM, Staines DG, Norris IM, De Frias R (2002); Friction stir welding-tools and developments, FSW Sem., Portugal, pp. 1-21.

[3] Mishra RS, Ma ZY (2005); Friction stir welding and processing, Materials Science and Engineering., 50, pp. 1-78.

[4] Galvao I, Oliveira JC, Loureiro (2011); Formation and distribution of brittle structures in friction stir welding of aluminium and copper: influence of process parameters", Science and Technology of Welding and Joining. 16, pp. 681-689.

[5] Mehta KP, Badheka VJ (2015); Influence of tool design and process parameters on dissimilar friction stir welding of copper to AA6061-T651 joints, International Journal of Advanced Manufacturing Technology, 80 (9), pp. 2073-2082.

[6] Venkateswaran P, Reynolds AP (2015); Factors affecting the properties of friction stir welds between aluminum and magnesium alloys, Materials Science and Engineering A., 545, pp. 26-37.

[7] Scialp A, Troughton M, Andrews S, Filippis De (2009); Friction stir welding for plastics, Welding International, 23(11), pp. 846-855.

[8] Colligan K (1999); Material flow behavior during friction stir welding of aluminum, The Welding Journal, pp. 229-237.

[9] Roy GG, Nandan R, Deb Roy T (2006); Dimensionless correlation to estimate peak temperature during friction stir welding, Science and Technology of Welding and Joining, 11(5), pp. 606-608.

[10] Bahemmat P, Haghpanahi M, Besharati MK, Ahsanizadeh S, Rezaei H (2010); Study on mechanical, micro-, and macrostructural characteristics of dissimilar friction stir welding of AA6061-T6 and AA7075-T6, Journal of Engineering and Manufacturing, 224(12), pp. 1854-1864.

[11] Bahemmat P (2012); Study on dissimilar friction stir butt welding of AA7075-O and AA2024-T4 considering the manufacturing limitation, International Journal of Advanced Manufacturing Technology, 59(9), pp. 939-95.

[12] Guo JF, Chen HC, Sun CN Bi G, Sun Z, Wei J (2014); Friction stir welding of dissimilar materials between AA6061 and AA7075 Al alloys effect of process parameters, Materials and Design, 56, pp. 185-192.

[13] Rodriguez RI, Jordon JB, Allison PG, Rushing T, Garcia L (2015); Microstructure and mechanical properties of dissimilar friction stir welding of AA6061-to-AA7050 aluminum alloys, Materials and Design, 83, pp. 60-65.

[14] Ilangovan M, Boopathy S, Balasubramanian V (2015); Effect of tool pin profile on microstructure and tensile properties of friction stir welded dissimilar AA 6061-AA 5086 aluminium alloy joints, Defense Technology, 11, pp. 174-184.

[15] Masoud A, Shahraki S (2016); Experimental studies on optimized mechanical properties while dissimilar joining AA6061 and AA5010 in a friction stir welding process, International Journal of Advanced Manufacturing Technology, 87(5), pp. 2337-2352.

[16] Ramanjaneyulu K, Madhusudhan Reddy G, Venugopal Rao A (2014); Role of tool shoulder diameter in friction stir welding: an analysis of the temperature and plastic deformation of AA 2014 aluminium alloy, Transactions of Indian Institute of Metals, 67, pp. 769-80.

[17] Venkateswara Rao R, Senthil Kumar M (2020); Effect of pin geometry on material flow characteristics of friction stir welded dissimilar AA6061/AA2014 alloys, Australian Journal of Mechanical Engineering, DOI:10.1080/14484846.2020.1723864.